Percolation in Yukawa fluids and clusters with a fractal structure

Tetsuo Kaneko*
Kurakenchikuzokeisha Company, Limited, Kita-ku Shimo, Tokyo 115-0042, Japan
(Received 16 October 1997; revised manuscript received 13 April 1998)

Extension in the effective range κ^{-1} of the attractive force does not vary the maximum depth of the Yukawa potential $u_{ij}^{Y}(r)$, so that a cluster consisting of particles linked as particle pairs satisfying the criterion $E(p_{ij})\leqslant -u_{ij}^{Y}(r)$ with the relative kinetic energy $E(p_{ij})$ cannot develop considerably as κ^{-1} increases. A tendency toward the generation of percolation resulting from such clusters is less dominant than that toward the aggregation of particles, resulting in only phase separation as κ^{-1} increases. The pair connectedness function for estimating such percolation can be expanded in powers of the pair potential. These powers include half-integer indices. As a result, it is predicted that clusters formed at least by the contribution of a sufficiently long-ranged attractive force can exhibit a fractal structure even in a Yukawa fluid. The structure has a fractal dimension of 1.5, which is near that for the cluster-cluster aggregation. [S1063-651X(98)07811-8]

PACS number(s): 61.43.Hv, 64.60.Ak

I. INTRODUCTION

Particular properties of a fluid can be influenced by clusters formed by the attractive force between particles constituting the fluid. Present interest will be focused on the generation of nonuniform states due to the formation of clusters created by the attractive force.

The electrical conductivity of liquid mercury maintained at low density at a temperature near the critical point, T_c, decreases with a rather steep gradient as the density of the mercury ρ_{H_g} decreases [1] The difference between the absorption of infrared at a particular density $\rho_{H_g}=\rho'_{H_g}$ and that at a density below ρ'_{H_g} increases as temperature decreases. This difference at temperatures lower than T_c is much larger than that near T_c [2]. For an H_g fluid near T_c, the real part of the dielectric constant determined using optical reflectivity and absorption measurements increases sharply at a particular density as ρ_{H_g} increases [3]. For inducing these phenomena, nonuniform fluid states resulting from the formation of clusters of H_g atoms in each H_g fluid can play a role. The lowest energy required for exciting an electron contributing to the formation of a cluster decreases toward zero as the number of metallic atoms constructing the cluster increases. The distribution of cluster sizes in a fluid consisting of metallic atoms is a factor which determines the dependence of optical absorption on the frequency of light [4].

Near liquid-vapor critical points, the viscosities of fluids exhibit asymptotic divergence. Berg and Moldover [5] determined the critical exponent characterizing the asymptotic divergence by measuring the viscosities of carbon dioxide and xenon near their critical points. In these fluids, the distribution of particles can never be uniform due to the large fluctuations in densities. Such fluctuations can result in anomalies for the electrical and optical properties of the H_g fluids. Similarly, the fluctuations can result in a characteristic increase in the viscosities of fluids near the critical points [6].

A factor enhancing the generation of the nonuniform distribution is the attractive force between particles which can drive the phase separation. The effective range of the attractive force contributes to the characteristics of the distribution. In fact, the effective range of the force can be an important factor that determines the liquid phase stability [7].

In order to include this factor in the present study, a bound state for a pair of i and j particles is defined as that satisfying the condition $E(p_{ij})\leqslant -u_{ij}(r)$, with the pair potential $u_{ij}(r)$ and relative kinetic energy $E(p_{ij})$.

An alternative definition given in Ref. [8] depends on the distance r between the i and j particles, and provides a bound state for a pair of i and j particles if r satisfies $r\leqslant r'$ for a particular value r'. The criterion $r\leqslant r'$ for the bound state is simple. However, it is difficult to distinguish the condition $E(p_{ij})> -u_{ij}(r)$ for $r\leqslant r'$ from the condition $E(p_{ij})\leqslant -u_{ij}(r)$ for $r\leqslant r'$. Therefore, the bound state defined by the criterion $r\leqslant r'$ provides a less satisfactory temperature dependence than that of the bound state defined by the criterion $E(p_{ij})\leqslant -u_{ij}(r)$. In the present work, such a difficulty is avoided, since the condition $E(p_{ij})\leqslant -u_{ij}(r)$ is applied as the criterion for defining the bound state.

Thus, a cluster resulting in the nonuniform distribution is assumed as an ensemble of particles joined as particle pairs satisfying the condition $E(p_{ij})\leqslant -u_{ij}(r)$. Such clusters can result in percolation [9]. In the present work, the dependence of such percolation on the effective range of the attractive force is studied. Using a Yukawa fluid, particular attention is paid to the dependence of the liquid phase stability on the effective range of the attractive force given by the pair potential [7]. Here, attention is focused on the dependence of the generation of the percolation state on the effective range of the attractive force.

The dependence of the generation of the percolation state on the effective range can be found by applying a heuristic percolation criterion to systems composed of core-soft-shell spheres with an attractive square-well potential [10]. For Yukawa fluids, the dependence of the generation of the percolation state on the effective range can be estimated by use of an adjustable parameter [11].

In order to simplify the estimate of the percolation based on the criterion $E(p_{ij})\leqslant -u_{ij}(r)$, an appropriate mathemati-

*Electronic address: kanekous@ppp.bekkoame.or.jp

cal treatment is required for solving the integral equation for the pair connectedness. The approximate treatment given in the present work is similar to the mean spherical approximation (MSA) for the Ornstein-Zernike equation and results in a simple estimate for the Yukawa fluids. However, the power of the pair potential in the closure for solving the integral equation differs from that in the closure for the MSA. The closure including the term $[u_{ij}(r)]^{3/2}$ is derived in Sec. III. To obtain analytical solutions for a Yukawa fluid, the closure must be approximated. Two approximations for the closure can be used. An approximation overestimates the decay of the closure due to the factor of $r^{-3/2}$. Another approximation overestimates the long-ranged contribution of the closure. In Sec. IV, it is demonstrated that the pattern of the phase diagrams resulting from the former is similar to that resulting from the latter. The pair connectedness in the present work exhibits the distribution of particles within a cluster where the particles are linked via bonds defined as bound states of pair particles satisfying the condition $E(p_{ij}) \leqslant -u_{ij}(r)$. To the creation of the cluster in a fluid, either particle-cluster aggregation or cluster-cluster aggregation contribute. If the distribution of the particles has a fractal structure, it may be a characteristic resulting from the cluster-cluster aggregation. According to the expansion of the pair connectedness to powers of a pair potential, the clusters generated in a Yukawa fluid can have a fractal structure when the attractive force is long-ranged. In Sec. V, it is demonstrated that a fractal dimension for the structure is close to that for the fractal structure resulting from cluster-cluster aggregation.

II. PAIR CONNECTEDNESS

The pair connectedness $P_{ij}(r)$ for estimating the percolation is introduced as the probability $\rho_i \rho_j P_{ij}(r) d\mathbf{r}_i d\mathbf{r}_j$ that both an i particle in a volume element $d\mathbf{r}_i$ and a j particle in a volume element $d\mathbf{r}_j$ belong to the same physical cluster. In the above, ρ_i and ρ_j are the densities of the i and j particles, respectively, for a uniform distribution. If a cluster has a fractal structure, $P_{ij}(r)$ should provide the characteristics of the fractal structure. If the probability that the i particle in $d\mathbf{r}_i$ and the j particle in $d\mathbf{r}_j$ do not belong to the same cluster is expressed as $\rho_i \rho_j D_{ij}(r) d\mathbf{r}_i d\mathbf{r}_j$, $P_{ij}(r)$ can be related to the pair correlation function $g_{ij}(r)$ as $g_{ij} = P_{ij} + D_{ij}$. Here, the physical meanings of P_{ij} and of D_{ij} require $\lim_{r\to\infty} P_{ij} = 0$ and $\lim_{r\to\infty} D_{ij} = 1$, since $\lim_{r\to\infty} g_{ij} = 1$.

On the other hand, to distingish between a bound state $E(p_{ij}) \leqslant -u_{ij}$ and an unbound state $E(p_{ij}) > -u_{ij}$ in the expression of $g_{ij}(r)$, which can be given using the grand partition function, the factor $\exp(-\beta u_{ij})$ is expressed as the sum of two factors given as

$$e^{-\beta u_{ij}} = p_b(r) e^{-\beta u_{ij}} + [1 - p_b(r)] e^{-\beta u_{ij}}, \tag{1}$$

where β is defined as $\beta \equiv 1/kT$. Here, k is Boltzmann's constant and T is the temperature. In Eq. (1), $p_b(r)$ (the so called pairwise bond probability) is the probability that a pair of i and j particles satisfies the condition $E(p_{ij}) \leqslant -u_{ij}$, so that $p_b(r)$ can be expressed as

$$p_b(r) = 2\pi^{-1/2} \int_0^{-\beta u_{ij}} y^{1/2} e^{-y} dy, \tag{2}$$

where $y = [\beta E(p_{ij})]^{1/2}$ [8]. If $-\beta u_{ij} < 0$, the probability must be $p_b(r) = 0$.

According to Eq. (1), the Mayer f function $f_{ij} = e^{-\beta u_{ij}} - 1$ is given as the sum of $f_{ij}^{+} \equiv p_b(r_{ij}) e^{-\beta u_{ij}}$ and $f_{ij}^{*} \equiv [1 - p_b(r_{ij})] e^{-\beta u_{ij}} - 1$. Using this sum, Mayer's mathematical clusters (diagrams defined in terms of f bonds) constituting g_{ij} can be expressed as those composed of f_{ij}^{+} (each f_{ij}^{+} is defined in terms of an f^{+} bond) and f_{ij}^{*}. The f^{+} bond corresponds to a pair of particles satisfying the condition $E(p_{ij}) \leqslant -u_{ij}$. If particles are joined by the f^{+} bonds, the ensemble of the particles forms a physical cluster. The physical cluster consists of the particles contributing to a diagram with at least one path of all the f^{+} bonds between the root points i and j, at which the i and j particles are located. Hence, the collection of such diagrams is that which contributes to P_{ij}.

The collection of diagrams contributing to P_{ij} can be separated into the sum of two parts, given by C_{ij}^{+} and N_{ij}^{+}. Here, the part C_{ij}^{+} is the contribution of non-nodal diagrams with at least one path of all f^{+} bonds between i and j. The part N_{ij}^{+} represents the contribution of nodal diagrams with at least one path of all f^{+} bonds between i and j. Hence, N_{ij}^{+} can be determined by the convolution integral of the product of C_{ij}^{+} and P_{ij}. Thus, P_{ij} can be expressed by an integral equation [9] having the same mathematical structure as the Ornstein-Zernike equation, as

$$P_{ij} = C_{ij}^{+} + \sum_{k=1}^{m} \rho_k \int C_{ik}^{+} P_{kj} d\mathbf{r}_k, \tag{3}$$

where m is the number of species.

III. APPROXIMATION SIMILAR TO MSA

For some fluids, analytical solutions of the Ornstein-Zernike equation can be obtained by considering the mean spherical approximation (MSA). In the MSA, the direct correlation function c_{ij} is given as the sum of the short-ranged and long-ranged contributions. Similarly, Eq. (3) could be solved simply if C_{ij}^{+} can be given as the sum of the short-ranged and long-ranged contributions.

Fortunately, the behavior of C_{ij}^{+} for a large distance between i and j can be readily determined. Using the contribution N_{ij} of the nodal diagrams for f bonds, the pair-correlation function g_{ij}^{PY} due to the Percus-Yevick (PY) approximation can be given by $g_{ij}^{\mathrm{PY}} e^{\beta u_{ij}} = 1 + N_{ij}$. Furthermore, N_{ij} can be separated into N_{ij}^{+} and a remainder N_{ij}^{*} (i.e., all nodal diagrams which do not include paths of all f^{+} bonds between i and j), so that the PY approximation is expressed as $g_{ij}^{\mathrm{PY}} = e^{-\beta u_{ij}}(1 + N_{ij}^{+} + N_{ij}^{*})$. If, with use of the above, the relations $P_{ij} = C_{ij}^{+} + N_{ij}^{+}$, $e^{-\beta u_{ij}} = f_{ij}^{+} + f_{ij}^{*} + 1$, and $g_{ij} = P_{ij} + D_{ij}$ are considered, g_{ij}^{PY} due to the PY approximation results in

$$P_{ij} = f_{ij}^{+} g_{ij}^{\mathrm{PY}} e^{\beta u_{ij}} + (f_{ij}^{*} + 1)(P_{ij} - C_{ij}^{+}) \tag{4a}$$

and

$$D_{ij}=f_{ij}^{*}+1+N_{ij}^{*}(f_{ij}^{*}+1)$$
$$=(f_{ij}^{*}+1)g_{ij}^{\mathrm{PY}}e^{\beta u_{ij}}-(f_{ij}^{*}+1)(P_{ij}-C_{ij}^{+}). \qquad (4b)$$

By considering $f_{ij}^{+}=p_b(r)e^{-\beta u_{ij}}$, $e^{-\beta u_{ij}}=f_{ij}^{+}+f_{ij}^{*}+1$, and the PY approximation $g_{ij}^{\mathrm{PY}}(1-e^{\beta u_{ij}})=c_{ij}^{\mathrm{PY}}$, Eq. (4a) can be rewritten as

$$P_{ij}+\frac{[1-p_b(r)]e^{-\beta u_{ij}}}{1-[1-p_b(r)]e^{-\beta u_{ij}}}C_{ij}^{+}=\frac{p_b(r)c_{ij}^{\mathrm{PY}}}{(1-e^{\beta u_{ij}})\{1-[1-p_b(r)]\}e^{-\beta u_{ij}}}. \qquad (5)$$

When the distance between i and j is sufficiently large, $|\beta u_{ij}|$ should be small. Equation (2) can then be given approximately as

$$p_b(r)=\frac{4}{3\sqrt{\pi}}(-\beta u_{ij})^{3/2}-\frac{4}{5\sqrt{\pi}}(-\beta u_{ij})^{5/2}+\frac{2}{7\sqrt{\pi}}(-\beta u_{ij})^{7/2}+\cdots.$$

The substitution of this approximation into Eq. (5) results in

$$C_{ij}^{+}=\frac{c_{ij}^{\mathrm{PY}}}{-\beta u_{ij}}\left(\frac{4}{3\sqrt{\pi}}(-\beta u_{ij})^{3/2}-\frac{22}{15\sqrt{\pi}}(-\beta u_{ij})^{5/2}+\cdots\right)+P_{ij}\left(-\beta u_{ij}-\frac{4}{3\sqrt{\pi}}(-\beta u_{ij})^{3/2}-\frac{1}{2}(-\beta u_{ij})^{2}+\frac{32}{15\sqrt{\pi}}(-\beta u_{ij})^{5/2}+\cdots\right).$$

If $c_{ij}^{\mathrm{PY}}/(-\beta u_{ij})=1$ for the MSA is substituted into this result, C_{ij}^{+} for $1\ll r$ can be given as $C_{ij}^{+}\approx 4/(3\sqrt{\pi})(-\beta u_{ij})^{3/2}$. Here, the condition $(-\beta u_{ij})P_{ij}\ll 4/(3\sqrt{\pi})(-\beta u_{ij})^{3/2}$ has been assumed for $1\ll r$.

For the PY approximation and the MSA, the correlation function g_{ij} satisfies the relation given as

$$\lim_{r\to\infty}\frac{g_{ij}-1}{-\beta u_{ij}}=\lim_{r\to\infty}\frac{1}{-\beta u_{ij}}\left(\frac{c_{ij}^{\mathrm{PY}}}{1-\exp(\beta u_{ij})}-1\right)=\frac{1}{2}.$$

The condition $P_{ij}/(g_{ij}-1)\leq 1$ is always satisfied, since $g_{ij}-1=P_{ij}+D_{ij}-1$. As a result, the magnitude of P_{ij} for $1\ll r$ should satisfy

$$\frac{g_{ij}-1}{-\beta u_{ij}}\geq\frac{P_{ij}}{-\beta u_{ij}}>\frac{P_{ij}}{(-\beta u_{ij})^{1/2}}.$$

Therefore, the following relation can be derived:

$$\frac{1}{2}>\lim_{r\to\infty}\frac{P_{ij}}{(-\beta u_{ij})^{1/2}}=0,$$

and the above assumption can provide validity.

Thus, an approximation similar to the MSA can be obtained for solving Eq. (3) as

$$C_{ij}^{+}=C_{ij}^{0+}+\frac{4}{3\sqrt{\pi}}(-\beta u_{ij})^{3/2}, \qquad (6)$$

where C_{ij}^{0+} is the short-ranged contribution. By considering that a hard-core potential resulting in the completely short-ranged interaction between i and j particles does not directly contribute to the interaction between them located beyond a particular distance σ_{ij}, it is assumed that

$$C_{ij}^{0+}(r)=0 \quad \text{for} \quad r\geq\sigma_{ij}, \qquad (7)$$

where σ_{ij} is given as $\sigma_{ij}=\frac{1}{2}(\sigma_i+\sigma_j)$ with the diameter σ_i of the hard core of the i particle and the diameter σ_j of the hard core of the j particle. If the short-ranged contribution C_{ij}^{0+} can be neglected for $r\geq\sigma_{ij}$, the mathematical treatment for Eq. (3) is considerably simplified, as it was in the MSA. As a result, the use of Eq. (7) can simplify the estimation of the percolation.

In order to solve Eq. (3) analytically for a fluid consisting of hard spheres interacting with the Yukawa potential given as

$$u_{ij}^{Y}(r)=-K_{ij}\frac{1}{r}\exp[-\kappa(r-\sigma_{ij})],$$

the long-ranged contribution in Eq. (6) must be somewhat modified as

$$C_{ij}^{+}(r)=C_{ij}^{0+}(r)+\hat{K}_{ij}\frac{e^{-zr}}{r}, \qquad (8a)$$

where

$$\hat{K}_{ij}\equiv\frac{4}{3\sqrt{\pi}}(\beta K_{ij})^{3/2}\sigma_{ij}^{-1/2}e^{z\sigma_{ij}}, \qquad (8b)$$

with

$$z\equiv\frac{1}{2}\left(3\kappa+\frac{1}{\sigma_{ij}}\right). \qquad (8c)$$

Here, $\hat{K}_{ij}$ and z are approximated by requiring the relation $4/(3\sqrt{\pi})[-\beta u_{ij}(r)]^{3/2}=\hat{K}_{ij}e^{-zr}/r$ for $0<r-\sigma_{ij}\ll 1$.

In addition, the above requirement results in an approximate expression given as

$$\frac{1}{r^{3/2}}=\frac{e^{1/2}}{\sqrt{\sigma_{ij}}}\frac{1}{r}\exp\left[-\frac{r}{2\sigma_{ij}}\right]. \qquad (9)$$

This means that the condition of $\kappa=0$ does not correspond to that of $z=0$ when the approximation is applied. Thus, on using the approximation given by Eq. (9), the decay of $C_{ij}^{+}(r)$ due to the factor of $r^{-3/2}$ can be somewhat overestimated.

IV. PERCOLATION THRESHOLD

Using Eq. (8a) and Baxter's Q function [12], Eq. (3) can be solved analytically [11]. If the calculations for the Orstein-Zernike equation [12–14] are considered, $P(r)$ and $C^{+}(r)$ satisfying Eq. (3) for a Yukawa fluid composed of a single component are given by

$$2\pi r P(r) = -\frac{d}{dr}Q(r) + 2\pi\rho\int_0^{\infty} Q(t)(r-t)P(|r-t|)dt \tag{10}$$

and

$$2\pi r C^{+}(r) = -\frac{d}{dr}Q(r) + \rho\int_0^{\infty} Q(t)\frac{d}{dr}Q(r+t)dt. \tag{11}$$

The function $Q(r)$ in Eqs. (10) and (11) is introduced as

$$\tilde{Q}(k) = 1-\rho\int_0^{\infty} e^{ikr}Q(r)dr \tag{12a}$$

and can be of the forms given by Eqs. (7) and (8a) as

$$Q(r) = (r-\sigma)\acute{q} + \check{C}(e^{-zr}-e^{-z\sigma}) + \check{D}e^{-zr} \quad (r<\sigma) \tag{12b}$$

and

$$Q(r) = \check{D}e^{-zr} \quad (\sigma \leqslant r). \tag{12c}$$

In Eqs. (12b) and (12c), σ is the diameter of the hard core of a particle. The unknown coefficients $\check{C}$, $\check{D}$, and $\acute{q}$ in Eqs. (12b) and (12c) can be determined using Eqs. (10) and (11).

If $\lim_{u_{ij}\to\infty} P_{ij} = 0$ due to Eq. (4) and Eq. (12b) are considered, Eq. (10) for $r<\sigma$ results in

$$-\acute{q} + z\check{C}e^{-zr} + z\check{D}e^{-zr} - 2\pi\rho\check{D}e^{-zr}\int_0^{\infty} P(t)e^{-zt}t\,dt = 0. \tag{13}$$

Thus, the relation between the left- and right-hand sides in Eq. (13) gives the restrictions for the coefficients as

$$\acute{q} = 0 \tag{14a}$$

and

$$\check{C} = -[1-\hat{P}(z)]\check{D}, \tag{14b}$$

where

$$\hat{P}(z) \equiv 2\pi\frac{\rho}{z}\int_0^{\infty} P(t)e^{-zt}t\,dt. \tag{14c}$$

By considering $C^{0+}(r)$ and Eq. (12c), Eqs. (8a) and (11) result in

$$2\pi\hat{K} = z\check{D} - z\rho\check{D}\hat{Q}(z), \tag{15}$$

where

$$\hat{Q}(s) \equiv \int_0^{\infty} Q(t)e^{-st}dt = \check{C}e^{-z\sigma}\left(\frac{e^{z\sigma}-e^{-s\sigma}}{s+z} - \frac{1-e^{-s\sigma}}{s}\right) + \check{D}\frac{1}{s+z}. \tag{16}$$

The expression given by Eq. (16) can be obtained by substituting Eq. (12b) into the integral.

On the other hand, Eq. (10) for $r<\sigma$ can be expressed as

$$0 = z\check{C}e^{-zr} + z\check{D}e^{-zr} + 2\pi\rho\int_r^{\infty} Q(t)(r-t)P(|r-t|)dt. \tag{17}$$

Equation (17) is equivalent to Eq. (13) which has no singularity for $0<r<\infty$, so that Eq. (17) is satisfied for $0<r<\infty$. Then, if each factor given by Eq. (17) is subtracted from each factor given by Eq. (10), a formula for $\sigma \leqslant r$ can be obtained as

$$2\pi r P(r) = -z\check{C}e^{-zr} + 2\pi\rho\int_0^{r} Q(t)(r-t)P(r-t)dt. \tag{18}$$

The Laplace transformation of Eq. (18) results in a relation between $\hat{P}(z)$ and $\hat{Q}(z)$ as

$$\frac{z}{\rho}\hat{P}(z)[1-\rho\hat{Q}(z)] = -\frac{1}{2}\check{C}e^{-2z\sigma}. \tag{19}$$

By considering Eq. (14b), the substitution of Eq. (16) into Eq. (15) results in

$$\frac{\check{D}}{\sigma^2} = \frac{\pi z\sigma}{6\phi} \times \frac{1-\left(1-\frac{24\phi}{(z\sigma)^2}\frac{\hat{K}}{\sigma}\{1-(1-e^{-z\sigma})^2[1-\hat{P}(z)]\}\right)^{1/2}}{1-(1-e^{-z\sigma})^2[1-\hat{P}(z)]}, \tag{20}$$

where ϕ is the volume fraction defined as

$$\phi \equiv \frac{\pi}{6}\rho\sigma^3.$$

On the other hand, by again considering Eq. (14b), the substitution of Eq. (16) into Eq. (19) yields

$$\frac{\check{D}}{\sigma^2} = \frac{\pi z\sigma}{3\phi} \times \frac{\hat{P}(z)}{e^{-2z\sigma} + 2\hat{P}(z)e^{-z\sigma}(1-e^{-z\sigma}) + [\hat{P}(z)]^2(1-e^{-z\sigma})^2}. \tag{21}$$

Using Eqs. (19) and (20), the unknown coefficients $\check{D}$ and $\hat{P}(z)$ can then be determined.

On using Baxter's Q function, the mean cluster size S [11] can be obtained as

$$S=[1-\rho\hat{Q}(0)]^{-2}. \tag{22}$$

Using Eqs. (14b) and Eq. (16), $\hat{Q}(0)$ can be determined as

$$z\hat{Q}(0)=-e^{-z\sigma}(e^{z\sigma}-1-z\sigma)[1-\hat{P}(z)]\check{D}+\check{D}. \tag{23}$$

By substituting Eq. (22) into Eq. (21), the mean cluster size S is given as

$$S=\left(1-\frac{6\phi}{\pi z\sigma}\frac{\check{D}}{\sigma^2}\{(1+z\sigma)e^{-z\sigma}+[1-(1+z\sigma)e^{-z\sigma}]\hat{P}(z)\}\right)^{-2}. \tag{24}$$

Therefore, the percolation threshold, at which $1-\rho\hat{Q}(0)=0$ should hold, can be estimated using the following equation:

$$\left[\frac{6\phi}{\pi z\sigma}\frac{\check{D}}{\sigma^2}\right]^{-1}-(1+z\sigma)e^{-z\sigma}-[1-(1+z\sigma)e^{-z\sigma}]\hat{P}(z)=0. \tag{25}$$

Equation (24) is derived from Eq. (23). The value of $\hat{P}(z)$ at the percolation threshold is obtained by substituting Eq. (20) into Eq. (24), as

$$\hat{P}^P=[(1-e^{-z\sigma})^2-2+2(1+z\sigma)e^{-z\sigma}]^{-1}\times e^{-z\sigma}\{z\sigma+e^{-z\sigma}-[(z\sigma+e^{-z\sigma})^2-(1-e^{-z\sigma})^2+2-2(1+z\sigma)e^{-z\sigma}]^{1/2}\}, \tag{26}$$

where $\hat{P}^P$ is the value of $\hat{P}(z)$ at the percolation threshold. If the value of $\hat{K}$ at the percolation threshold is exressed as $\hat{K}^P$, the value of $\hat{K}^P$ can be obtained by modifying Eq. (19) as

$$\frac{\hat{K}^p}{\sigma}=\frac{z\sigma}{2\pi}\frac{\check{D}^P}{\sigma^2}-\frac{3\phi}{2\pi^2}[1-(1-e^{-z\sigma})^2(1-\hat{P}^P)]\left(\frac{\check{D}^P}{\sigma^2}\right)^2, \tag{27}$$

where $\check{D}^P$ is the value of $\check{D}$ evaluated from Eq. (20) for $\hat{P}(z)=\hat{P}^P$. If Eq. (8b) is considered as the relation between K and $\hat{K}$, the substitution of Eq. (20) into Eq. (27) results in a relation expressed as $1/K^P\propto\phi^\nu$ with $\nu=2/3$. Here, K^P is the value of K at the percolation threshold. The relation $1/K^P\propto\phi^\nu$ with $\nu=1$ corresponds to that given by Xu and Stell [11].

The percolation thresholds evaluated using Eq. (26) with Eqs. (8b) and (8c) are represented for each Yukawa fluid ($\kappa\sigma=0.2,0.8,3,7.5,25$) in Fig. 1. The percolation threshold for $\kappa\sigma=3$ demonstrates that the state of no percolation in the liquid phase can be induced when ϕ is small. This phenomenon is similar to that found from the phase diagram in Ref. [9]. The phenomenon suggests that a state of low viscosity due to the lack of percolation induced in the liquid phase can change to another state of high viscosity due to the percolation as ϕ increases.

If the contribution of the attractive force between particles generates the liquid phase even when the effective range κ^{-1} is narrow, particles in the liquid phase should be close to each other. For the generation of the liquid phase, sufficiently dense parts at least must be formed in the fluids. These dense parts can correspond to high-density regions formed as clusters due to the percolation criterion used in the present work. On the other hand, particles also must be close to each other in order to induce the percolation, if κ^{-1} is small. Therefore, it is expected that the percolation state may always be found in the liquid phase, if the liquid phase is generated even when κ^{-1} is small. This phenomenon is demonstrated by the diagrams given for $\kappa\sigma=7.5$ and 25 in Fig. 1.

Thus, it is inferred that the liquid phase contains extremely large clusters, if the liquid phase is generated in a fluid consisting of particles interacting with a short-ranged attractive force. Conversely, if κ^{-1} is not small, the generation of the liquid phase does not require clusters of extremely large size, since particles should readily be retained in the liquid phase due to the attractive force contributing over a long range.

Moreover, the percolation thresholds given in Fig. 1 demonstrate that the volume fraction ϕ at the percolation threshold for a particular value of K decreases as the effective range κ^{-1} is extended. Behavior similar to this has been found in a percolating system composed of core-soft-shell spheres with an attractive square-well potential [10].

If the effective range κ^{-1} is extended, overlaps of the effective range due to each particle increase. The number of particles with which a particle interacts increases as the overlaps of the effective range increase, so the increase in κ^{-1} can enhance a cooperative effect which contributes to the formation of the nonuniform particle distribution. Thus, either the generation of the percolation or the aggregation of

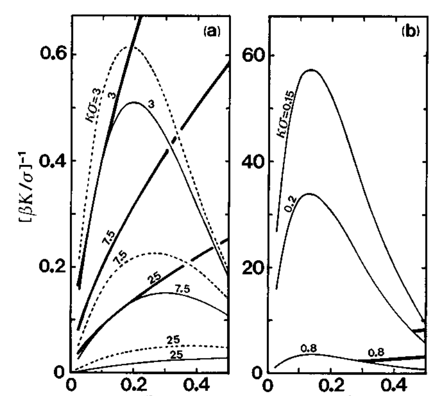

FIG. 1. The dependence of percolation on κ given by $[\kappa\sigma=(2z\sigma-1)/3]$ in the Yukawa fluids. The thick solid curves are the loci of the percolation thresholds. The dashed curves are the loci of points for which the compressibility is infinite, and have been evaluated on the basis of Ref. [15]. The thin solid curves are the loci of the points in a lower region for which no real solution can be obtained for the Ornstein-Zernike equation for a fluid, and have been evaluated on the basis of Ref. [13]. In (b), no dashed curve exists. In addition, $(\beta K/\sigma)^{-1}$, $\kappa\sigma$, and ϕ are dimensionless.

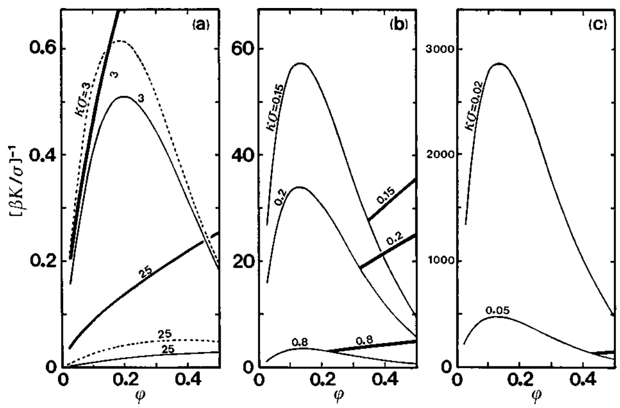

FIG. 2. Same as in Fig. 1, except for $\kappa\sigma = 2z\sigma/3$.

particles resulting in only the phase separation can be enhanced as κ^{-1} increases. It is, however, expected that the tendency toward the generation of percolation is less dominant than that toward the aggregation resulting in only phase separation. In the distribution of particles surrounding an i particle, particles satisfying the criterion $E(p_{ij}) \leqslant u_{ij}(r)$ should not increase considerably as κ^{-1} increases, since the increase in κ^{-1} does not deepen the Yukawa potential. The phenomenon discussed here can be recognized in Fig. 1. In addition, it must be considered that $[\beta K^P/\sigma]^{-1}$ given for small values of $\kappa\sigma$ in Fig. 1 can be somewhat too small.

On applying the Yukawa potential to Eq. (6), the decrease in $C_{ij}^{+}(r)$ due to the factor $(e^{-\kappa r})^{3/2}$ can be much more dominant than that due to the factor $(1/r)^{3/2}$, as r increases. Considering this, the contribution from the factor $(1/r)^{3/2}$ can be approximated by $1/r$ in Eq. (6). As a result, an alternative approximation for $[-\beta u_{ij}(r)]^{3/2}$ can be given as

$$\frac{4}{3\sqrt{\pi}}[-\beta u_{ij}(r)]^{3/2} = \frac{4}{3\sqrt{\pi}} \frac{(\beta K_{ij})^{3/2}}{\sigma_{ij}^{1/2}} \frac{1}{r} \exp[-\tfrac{3}{2}\kappa(r-\sigma_{ij})], \tag{28a}$$

so that z must be estimated as

$$z = \tfrac{3}{2}\kappa. \tag{28b}$$

This approximation somewhat overestimates the long-ranged contribution of $C_{ij}^{+}(r)$, since the contribution of $(1/r)^{3/2}$ is approximated as $(1/\sigma_{ij}^{1/2})(1/r)$. Thus, z given by Eq. (28b) differs from z given by Eq. (8c). This difference is considerable when $\kappa\sigma$ is small. When z is given as Eq. (28b) instead of Eq. (8c), the percolation in each Yukawa fluid ($\kappa\sigma$=0.02,0.05,0.15,0.2,0.8,3,25) behaves as shown in Fig. 2. The values of $[\beta K/\sigma]^{-1}$ at the percolation threshold given in Fig. 2 are larger than those at the percolation threshold given in Fig. 1. This tendency develops as $1/\kappa\sigma$ increases.

The behavior of the percolation threshold described above means that an overestimate for the long-ranged contribution of $C_{ij}^{+}(r)$ can lead to an overestimate for $[\beta K^P/\sigma]^{-1}$. When the decay of $C_{ij}^{+}(r)$ due to the increase in r is overestimated, the value of $[\beta K^P/\sigma]^{-1}$ is smaller than that for overestimating the long-ranged contribution. However, the diagrams representing the percolation behavior in Fig. 2 have the same pattern as those in Fig. 1. The maximum point at which the Ornstein-Zernike equation for a fluid results in a real solution shifts to an upper position in each phase diagram as $1/\kappa\sigma$ increases. Such a shift can exceed the shift of the percolation threshold for large values of $1/\kappa\sigma$. The overestimate for the decay of $C_{ij}^{+}(r)$ due to Eq. (8c) does not cause the pattern of the diagrams in Fig. 1 to be derived. Therefore, it is inferred that the tendency toward the generation of percolation is less dominant than that toward the aggregation, resulting in only the phase separation as $1/\kappa\sigma$ increases.

V. THREE PARAMETERS

The number n_{pair} of particle pairs satisfying the bound condition defined by the inequality $E(p_{ij}) \leqslant -u_{ij}^{Y}(r)$ can increase as K increases. Moreover, n_{pair} can increase, both as κ^{-1} increases and as ϕ increases. The variations in K, κ^{-1}, and ϕ can result in variations in $P(r)$ and in $g(r)$ due to the change in n_{pair}. Then, the behavior of $P(r)$ and $g(r)$ due to the variation in K can differ from that due to the variation in κ^{-1}, since the increase in K can enhance the magnitude of $-u_{ij}^{Y}(r)$ in the range $0 < r-\sigma \ll 1$, while the variation in κ^{-1} cannot change it in the range. Similarly, the behavior of $P(r)$ and $g(r)$ due to the variation in ϕ can differ from that due to the variation in K. Without changes in $-u_{ij}^{Y}(\sigma)$, increases in κ^{-1} as well as in ϕ lead to an increase in the number of particles with which a particle interacts. Thus, the behavior of $P(r)$ and $g(r)$ due to the increases in either κ^{-1} or ϕ may differ from that due to the increase in K.

Fortunately, $P(r)$ can be estimated readily in the range $0 < r-\sigma \ll 1$. If Eqs. (14b) and (18) are used with $\lim_{u_{ij}\to\infty} P_{ij} = 0$ due to Eq. (4), it is given as

$$2\pi\sigma P(\sigma^{+}) = z e^{-z\sigma}[1-\hat{P}(z)]\check{D},$$

where $P(\sigma^{+}) \equiv \lim_{\delta\to 0} P(\sigma+\delta)$.

The pair correlation function $g(r)$ for $0 < r-\sigma \ll 1$ can be given on the basis of Ref. [13] as

$$g(\sigma^{+}) = g^{\text{HS}} + \frac{\beta K}{\sigma}[F_0(\kappa\sigma,\phi) + \kappa\sigma X F_1(\kappa\sigma,\phi)]^{-2},$$

where

$$g^{\text{HS}} = \frac{1}{1-\phi}\left(1 + \frac{2\phi}{1-\phi}\right),$$

$$F_0(\kappa\sigma,\phi) = 1 + \frac{1}{\kappa\sigma}(1-e^{-\kappa\sigma})\frac{3\phi}{1-\phi} - \frac{4}{(\kappa\sigma)^3}\left[1 - \frac{\kappa\sigma}{2} - \left(1+\frac{\kappa\sigma}{2}\right)e^{-\kappa\sigma}\right] \times \frac{3\phi}{1-\phi}\left(1 + \frac{\kappa\sigma}{2} + \frac{3\phi}{1-\phi}\right),$$

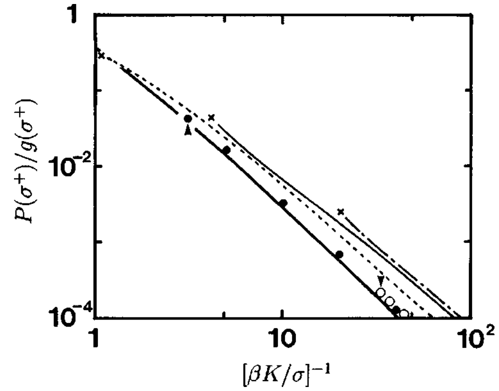

FIG. 3. The ratio $P(\sigma^+)/g(\sigma^+)$ as a function of $(\beta K/\sigma)^{-1}$ for the Yukawa fluids. To evaluate, Eqs. (8b) and (28b) are used for the relation between K and $\hat{K}$. The solid curve is determined for $\kappa\sigma=3$ and $\phi=0.1$. Points indicated by the solid circles (●) are determined for $\kappa\sigma=0.8$ and $\phi=0.1$. Points represented by open circles (○) are determined for $\kappa\sigma=0.2$ and $\phi=0.1$. The dashed line with a point indicated by the symbol (×) is determined for $\kappa\sigma=3$ and $\phi=0.35$. The thin solid line with a point indicated by the symbol (×) is determined for $\kappa\sigma=0.8$ and $\phi=0.35$. The dot-dash line with a point indicated by the symbol (×) is determined for $\kappa\sigma=0.2$ and $\phi=0.35$. Each point indicated by the symbol (×) expresses the percolation threshold. Each point denoted by an arrow expresses the maximum point at which the Ornstein-Zernike equation for a fluid results in a real solution.

$$F_1(\kappa\sigma,\phi)=\frac{1}{\kappa\sigma}(1-e^{-\kappa\sigma})-\frac{4}{(\kappa\sigma)^3}\left[1-\frac{\kappa\sigma}{2}-\left(1+\frac{\kappa\sigma}{2}\right)e^{-\kappa\sigma}\right]\frac{3\phi}{1-\phi},$$

and

$$X(X+1)\left(X+\frac{F_0(\kappa\sigma,\phi)}{\kappa\sigma F_1(\kappa\sigma,\phi)}\right)^2=-\frac{\beta K}{\sigma}\frac{6\phi}{[(\kappa\sigma)^2F_1(\kappa\sigma,\phi)]^2}.$$

In Fig. 3, the behavior described above can be recognized as that of the ratio $P(r)/g(r)$ in the range $0<r-\sigma\ll 1$. While the ratio $P(\sigma^+)/g(\sigma^+)$ increases as K increases, it hardly changes for the variations in either κ^{-1} or ϕ when the values of κ^{-1} and σ fall in the particular ranges.

Furthermore, when $P(r)/D(r)$ is given at least in the range $0<r-\sigma\ll 1$, its behavior can be considerably insensitive to variations in either κ^{-1} or ϕ, if the values of κ^{-1} and ϕ fall in the particular ranges. The ratio $P(r)/D(r)$ can be related to $P(r)/g(r)$ using $P(r)/g(r)=[1+D(r)/P(r)]^{-1}$. Here, $D(r)$ is given by Eq. (4b), and expresses the partial distribution of particles surrounding a particle. Then the particles resulting in the partial distribution described by $D(r)$ do not belong to the cluster to which the particle belongs.

Particles in a shell surrounding a particular particle and having a certain thickness can be divided into two groups. One group consists of N_1 particles which belong to a cluster with the particle. The other group consists of N_2 particles belonging to clusters to which the particle does not belong. Extension in the effective range κ^{-1} of the attractive force can result in increases in both N_1 and N_2. However, the extension does not vary the maximum depth of the Yukawa potential, so that N_1 cannot increase considerably as κ^{-1} increases. As a result, it is expected that the increase in N_2 is more dominant than that in N_1 as κ^{-1} increases. This is demonstrated in Fig. 3. According to Fig. 3, the value of $P(\sigma^+)/g(\sigma^+)$ at the percolation threshold decreases as κ^{-1} increases. This means that the ratio N_2/N_1 near the particle increases as κ^{-1} increases, since $g(\sigma^+)$ is equal to $P(\sigma^+)+D(\sigma^+)$.

The increase in N_2/N_1 can suppress the development of clusters. As a result, if κ^{-1} is sufficiently large, sizes of the clusters in the fluid remain small while the fluid falls in a state where it can undergo the phase separation. Thus, it is inferred that owing to the increase in N_2/N_1, the tendency toward the generation of percolation is less dominant than that toward aggregation, resulting in only phase separation as κ^{-1} increases.

On the other hand, the ratio $P(\sigma^+)/g(\sigma^+)$ at the percolation threshold increases as the effective range κ^{-1} decreases. This means that the number of particles must be large near each particle to induce the percolation if the effective range is narrow. This phenomenon is reasonable.

VI. FRACTAL STRUCTURE

If clusters can be found in Yukawa fluids, it is predicted that the clusters can have a fractal structure in the range of r where both $-\beta u(r)\ll 1$ and $\exp[-\kappa(r-\sigma_{ij})]\sim 1$ can be satisfied. When the magnitude of $(\beta K/\sigma)^{-1}$ is large, $-\beta u(r)$ is small, even for $r=\sigma$. If $\kappa\sigma$ is small, the magnitude of $(\beta K/\sigma)^{-1}$ at the percolation threshold is large as shown in Fig. 1 (Fig. 2). Hence, the clusters can be formed even when $-\beta u(r)$ is small, if $\kappa\sigma$ is small. By considering this, the expansion of Eq. (5) in powers of $-\beta u_{ij}$ results in

$$P_{ij}=-\frac{c_{ij}^{\rm PY}}{-\beta u_{ij}}\left[\frac{4}{3\sqrt{\pi}}(-\beta u_{ij})^{1/2}+\frac{16}{9\pi}(-\beta u_{ij})+\left(\frac{64}{27\pi^{3/2}}-\frac{4}{5\sqrt{\pi}}\right)(-\beta u_{ij})^{3/2}+\cdots\right]+\frac{C_{ij}^{+}}{-\beta u_{ij}}\left[1+\frac{4}{3\sqrt{\pi}}(-\beta u_{ij})^{1/2}+\left(\frac{1}{2}+\frac{16}{9\pi}\right)(-\beta u_{ij})+\cdots\right].$$

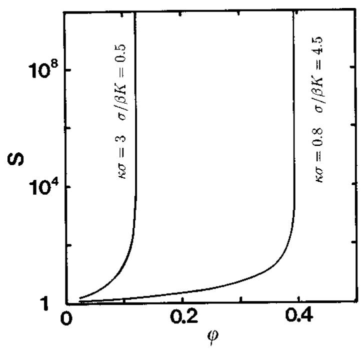

FIG. 4. The increases in S due to the increase in the volume fraction ϕ. The values of ϕ at the percolation thresholds are given as $\phi \approx 0.115, 0.394$. In addition, S is dimensionless.

If the approximation given by Eqs. (6) and (7) and $c_{ij}^{\mathrm{PY}}/(-\beta u_{ij})=1$ for the MSA are considered in this expansion, the result can be expressed as

$$P_{ij} \sim (-\beta u_{ij})^{3/2}. \tag{29}$$

Hence, in the range of r where $\exp[-\kappa(r-\sigma_{ij})]\sim 1$ can be satisfied, the pair connectedness $P(r)$ for the Yukawa potential can behave as

$$P(r) \sim r^{-\alpha}, \quad \alpha = 1.5. \tag{30}$$

In the range of r where $\exp[-\kappa(r-\sigma_{ij})]\sim 1$ can be satisfied, $P(r)$ can decay with $r^{-\alpha}$ having a noninteger index α. The pair connectedness gives the average characteristics of the particle distribution in a cluster. Therefore, it is predicted that clusters resulting in a nonuniform fluid can have a fractal structure with the fractal dimension $1.5(=3-\alpha)$ due to Eq. (30). This fractal dimension is close to a known fractal dimension (i.e., $d_f \sim 1.75$) for the fractal structure resulting from cluster-cluster aggregation [16]. As far as Yukawa fluids are concerned, the structure of a cluster can be fractal at least in the range of r where both $-\beta u(r) \ll 1$ and $\exp[-\kappa(r-\sigma_{ij})]\sim 1$ can be satisfied.

Then, this range should fall within the extent of the cluster of particles. This requirement is satisfied by the percolating clusters. Also, it can be satisfied even near the percolation thresholds, since clusters can have large sizes near the percolation thresholds as seen in Fig. 4.

The range of r where $\exp[-\kappa(r-\sigma_{ij})]\sim 1$ can be satisfied is more extensive if $\kappa\sigma$ is smaller. Moreover, the magnitude of $(\beta K/\sigma)^{-1}$ at the percolation threshold is large if $\kappa\sigma$ is small. In this case, it is inferred that the fractal structure of clusters can develop considerably, if the effective range κ^{-1} is extensive.

VII. CONCLUSIONS

A bond between particles is defined as a bound state between them using the criterion $E(p_{ij}) \leqslant -u_{ij}(r)$. A cluster is regarded as the distribution of particles linked via such bonds. The structure linked via the bonds can have a fractal structure with the fractal dimension 1.5. This value is close to a fractal dimension for the fractal structure resulting from cluster-cluster aggregation.

The pair connectedness relevant to the distibution can be given by the integral equation. If the closure given in the present work is used, the integral equation can be solved somewhat readily. Using the integral equation and the closure, analytical estimations of percolation can be obtained readily for a Yukawa fluid although the dependence of the closure on r must be approximated. One approximation is given as the overestimation for the decay of the closure due to the factor of $r^{3/2}$. Another approximation is given as the overestimation for the long-ranged contribution of the closure. Fortunately, the percolation behavior resulting from the former is similar to that resulting from the latter. However, the values of $[\beta K/\sigma]^{-1}$ at the percolation threshold given by the former are smaller than those given by the latter. This tendency develops as $1/\kappa\sigma$ increases.

Extension in the effective range κ^{-1} enhances the formation of the nonuniform particle distribution, and can result in dense parts and rare parts. In the dense parts, the increase in the number of particles which do not satisfy the condition $E(p_{ij}) \leqslant -u_{ij}(r)$ for a particular particle (e.g., an i particle) can exceed the increase in the number of particles satisfying the condition $E(p_{ij}) \leqslant -u_{ij}(r)$ for the particle, if the effective range extends sufficiently. If an effect resulting from the former is considerable, the dense parts can be regarded as an ensemble of small clusters. Therefore, a tendency toward the generation of percolation can be less dominant than that toward the aggregation, resulting in only phase separation as κ^{-1} increases.

In addition, the structure linked via the bonds defined by the criterion $E(p_{ij}) \leqslant -u_{ij}(r)$ can develop the fractal structure as κ^{-1} increases.

[1] G. Schönherr, R. W. Schmutzler, and F. Hensel, Philos. Mag. B **40**, 411 (1979).
[2] H. Uchtmann, F. Hensel, and H. Overhof, Philos. Mag. B **42**, 583 (1980).
[3] W. Hefner and F. Hensel, Phys. Rev. Lett. **48**, 1026 (1982).
[4] R. N. Bhatt and T. M. Rice, Phys. Rev. B **20**, 466 (1979).
[5] R. F. Berg and M. R. Moldover, J. Chem. Phys. **93**, 1926 (1990).
[6] J. K. Bhattacharjee and R. A. Ferrell, Phys. Rev. A **28**, 2363 (1983).
[7] M. H. J. Hagen and D. Frenkel, J. Chem. Phys. **101**, 4093 (1994).
[8] T. L. Hill, *Statistical Mechanics* (Dover, New York, 1987).
[9] A. Coniglio, U. De Angelis, and A. Forlani, J. Phys. A **10**, 1123 (1977).
[10] U. Alon, I. Balberg, and A. Drory, Phys. Rev. Lett. **66**, 2879 (1991).
[11] J. Xu and G. Stell, J. Chem. Phys. **89**, 1101 (1988).
[12] R. J. Baxter, J. Chem. Phys. **52**, 4559 (1970).
[13] M. Ginoza, J. Phys.: Condens. Matter **6**, 1439 (1994).
[14] L. Blum and J. S Hø ye, J. Stat. Phys. **19**, 317 (1978).
[15] P. T. Cummings and E. R. Smith, Chem. Phys. **42**, 241 (1979); Mol. Phys. **38**, 997 (1979).
[16] T. Vicsek, *Fractal Growth Phenomena* (World Scientific, New Jersey, 1992).